

Dynamics of hadron strong production and decay

T. J. Burns,^{*} F. E. Close,[†] and C. E. Thomas[‡]

Rudolf Peierls Centre for Theoretical Physics, University of Oxford, 1 Keble Road, Oxford, OX1 3NP, United Kingdom

(Received 5 October 2007; published 14 February 2008)

We generalize results of lattice QCD to determine the spin-dependent symmetries and factorization properties of meson production in Okubo-Zweig-Iizuka allowed processes. This explains some conjectures previously made in the literature about axial meson decays and gives predictions for exclusive decays of vector charmonia, including ways of establishing the structure of $Y(4260)$ and $Y(4325)$ from their S -wave decays. Factorization gives a selection rule which forbids $e^+e^- \rightarrow D^*D_2$ near threshold with the tensor meson in helicity 2. The relations among amplitudes for double charmonia production $e^+e^- \rightarrow \psi + \chi_{0,1,2}$ are expected to differ from the analogous relations among light flavor production such as $e^+e^- \rightarrow \omega f_{0,1,2}$.

DOI: [10.1103/PhysRevD.77.034008](https://doi.org/10.1103/PhysRevD.77.034008)

PACS numbers: 12.39.Jh, 13.25.Gv

I. INTRODUCTION

The dynamics of strong decay amplitudes are poorly understood. Definitive answers are not known to questions as basic as (i) are the $q\bar{q}$ created in an Okubo-Zweig-Iizuka allowed decay spin singlet or spin triplet; (ii) what is their overall J^{PC} ; and (iii) are the $q\bar{q}$ created from the energy of the strong confinement field, or from a hard gluon? It is our purpose in this paper to address these questions. We shall show that results from lattice QCD imply that light $q\bar{q}$ pair has spin 1 with an effective factorization of constituent spin and orbital degrees of freedom such that the $q\bar{q}$ in the initial meson are passive spectators. By contrast, if heavy flavors are created, as in $e^+e^- \rightarrow \psi + \chi_J$, factorization is broken with spin and momentum transferred from the initial $c\bar{c}$ to the created pair, such as by a hard gluon. This implies a radically different spin dependence of amplitudes, and of angular distributions, in analogue processes such as $e^+e^- \rightarrow \omega f_2$ relative to $e^+e^- \rightarrow \psi \chi_2$.

While lattice QCD is now a mature guide for the masses of glueballs and hybrids, at least in the quenched approximation [1,2], it is not yet mature enough to determine hadronic decays extensively. Consequently, at a fundamental level the dynamics of such decays is not yet established. Flux-tube models of both spectra [3,4] and decays [5,6] have been developed, in part stimulated by attempts to model the lattice, and lattice work has confirmed their spectroscopy [2,4]. The lattice is now beginning to confirm aspects of the flux-tube model for some decays: specifically, the lattice QCD studies of the decays of hybrid $1^{-+} \rightarrow \pi b_1$ and πf_1 [7] show quantitative features that were anticipated in flux-tube models [5,6], and in Ref. [8] we showed that these approaches exhibit remarkable agreement when compared under the same kinematic conditions. Specifically, for S -wave decay amplitudes at zero

recoil the results are consistent with

$$a(\pi_1 \rightarrow \pi + b_1[{}^1P_1]) = 2a(\pi_1 \rightarrow \pi + f_1[{}^3P_1]), \quad (1)$$

where π_1 denotes the first gluonic excited hybrid with $J^{PC} = 1^{-+}$.

In Sec. II we describe the underlying assumptions of the factorization hypothesis: (i) the hadrons' spins, j , separate into two parts—the intrinsic spins of the constituents s and a residual component that transforms as angular momentum l , (ii) the l and s degrees of freedom act independently throughout the transition (“factorization”), and (iii) the $q\bar{q}$ pair produced has spin 1. In Sec. II A we demonstrate that the above ratio is immediate within the factorization hypothesis. We identify further implications of factorization for the decays of axial and vector mesons in Secs. II B and II C; the former confirms and explains a conjecture of [9] and the latter has implications for charmed meson production from a $\psi({}^3S_1)$ initial state. A helicity selection rule is derived implying that in $e^+e^- \rightarrow D^*D_2$ near threshold or from a $\psi({}^3S_1)$ initial state the D_2 cannot be produced with helicity 2. In Sec. II D we apply the results of factorization to the decays of $c\bar{c}$ to charmed mesons near threshold in relative S waves, and identify ways to distinguish between hybrid and conventional interpretations of enigmatic ψ -like states such as $Y(4260)$ or $Y(4325)$.

In Sec. III we discuss application to e^+e^- annihilation for light and heavy flavors. We show that decays triggered by hard gluons violate factorization, and that emerging data on $e^+e^- \rightarrow \psi + \chi_j$ appear to support this. We propose tests for factorization and hard gluon production mechanisms in $e^+e^- \rightarrow \psi + \chi_j$ near threshold.

II. FACTORIZATION: FORMULATION AND APPLICATION

Our approach to strong decays is similar in spirit to what was done in the past decades for electromagnetic and current induced transitions among hadrons, known variously as Melosh transformation or more generally “single

^{*}burns@thphys.ox.ac.uk

[†]F.Close1@physics.ox.ac.uk

[‡]C.Thomas1@physics.ox.ac.uk

quark transition algebra” [10]. The empirically successful hypothesis there was that the interaction of a current with a single quark triggers a transition, all other constituents being passive spectators. That led to algebraic relations among amplitudes, which arose from the Clebsch-Gordan coefficients coupling the orbital, spin, and total angular momentum projections l_z, s_z to j_z for the initial and final hadrons, and the l_z, s_z algebraic transformation properties of the transition operators. While the relative strengths of the reduced matrix elements associated with each transition operator are, in this general approach, undetermined, the experimentally accessible range of helicity amplitudes for photo-excitation of proton and neutron targets to different resonances within a supermultiplet led to experimentally testable relations among various amplitudes [11]. Within the hypothesis of l, s factorization, analogous relations arise for strong decays. Specific models have implicitly assumed such factorization [5,6,12–14]; we shall see that the results from lattice QCD suggest that this property is realized in decays, at least for light flavors.

We consider the decay process of mesons $M \rightarrow M_1 + M_2$. In meson M with spin j , the $q\bar{q}$ have spin s and residual angular momentum l . We illustrate the structure of the amplitude for the particular case of a flux tube that breaks to form a new $q\bar{q}$ in a 3P_0 configuration leading to a pair of mesons M_1, M_2 with spins j_1, j_2 , respectively, and their $q\bar{q}$ having s_1, l_1, s_2, l_2 . The generalization will be immediate.

The width for the decay of a meson into a pair of mesons involves a sum over couplings of $j_1 \otimes j_2$ to j_{12} and relative

partial waves L :

$$\begin{aligned} & \Gamma(slj \rightarrow s_1 l_1 j_1 + s_2 l_2 j_2) \\ & \sim \sum_{j_{12} L} \langle (((s_1 \otimes l_1)_{j_1} \otimes (s_2 \otimes l_2)_{j_2})_{j_{12}} \otimes L)_j \| \sigma \cdot \nabla \| (s \otimes l)_j \rangle^2 \end{aligned} \quad (2)$$

where σ transforms as a vector in spin space and ∇ acts on the spatial (orbital and radial) degrees of freedom. Usually at this point specific wave functions are assumed and non-relativistic expressions calculated for the amplitudes [5,6,12–14]. However, this introduces model dependence and obscures the more general underlying properties. Instead, we shall factor the amplitude in such a way that the spin and space parts are separated [15], expressing all decay amplitudes as linear combinations of model-dependent spatial amplitudes, which in the present work are left general.

The first step is to separate the spin and space degrees of freedom of the final state. The final state bra

$$\langle (((s_1 \otimes l_1)_{j_1} \otimes (s_2 \otimes l_2)_{j_2})_{j_{12}} \otimes L)_j | \quad (3)$$

is recoupled to form states of good (s_{12}, l_{12}, l_f) :

$$\langle ((s_1 \otimes s_2)_{s_{12}} \otimes ((l_1 \otimes l_2)_{l_{12}} \otimes L)_{l_f})_j | \quad (4)$$

which involves a product of 6- j and 9- j coefficients. The spin and space parts then factorize and can be isolated. The result is

$$\begin{aligned} & \langle (((s_1 \otimes l_1)_{j_1} \otimes (s_2 \otimes l_2)_{j_2})_{j_{12}} \otimes L)_j \| \sigma \cdot \nabla \| (s \otimes l)_j \rangle \\ & = \sum_{s_{12} l_{12} l_f} (-)^{s+L+s_{12}+l_{12}+l_f} \Pi_{l_f s_{12} l_{12} j_1 j_2 j_{12}} \begin{Bmatrix} s_1 & l_1 & j_1 \\ s_2 & l_2 & j_2 \\ s_{12} & l_{12} & j_{12} \end{Bmatrix} \begin{Bmatrix} s_{12} & l_{12} & j_{12} \\ L & j & l_f \end{Bmatrix} \begin{Bmatrix} s_{12} & s & 1 \\ l & l_f & j \end{Bmatrix} \\ & \times \langle (s_1 \otimes s_2)_{s_{12}} \| \sigma \| s \rangle \langle ((l_1 \otimes l_2)_{l_{12}} \otimes L)_{l_f} \| \nabla \| l \rangle \end{aligned} \quad (5)$$

with

$$\Pi_{ab\dots} = \sqrt{(2a+1)(2b+1)\dots} \quad (6)$$

The spin part is a 9- j coefficient along with appropriate counting factors

$$\langle (s_1 \otimes s_2)_{s_{12}} \| \sigma \| s \rangle = (-)^{s+s_1} \Pi_{1s s_1 s_2 s_{12}} \begin{Bmatrix} \frac{1}{2} & \frac{1}{2} & s_1 \\ \frac{1}{2} & \frac{1}{2} & s_2 \\ s & s & s_{12} \end{Bmatrix}. \quad (7)$$

The 9- j coefficient in Eq. (7) is zero for $s_1 = s_2 = s = 0$; this is the well-known spin-singlet selection rule and is a consequence of the orthogonality of the spin wave functions. Note in the above that a phase of (-1) has been included for the permutation of quark and antiquark op-

erators [9], and the expression (5) is equivalent to that in Ref. [16].

The assumption driving the expansion of Eq. (5) is that the angular momentum and spin quantum numbers factorize and that the decay operator is overall scalar with a spin-triplet part. The angular momentum algebra makes no reference to the spatial part of the operator; hence the linear combinations for 3P_0 and 3S_1 decay models, driven by operators $\sigma \cdot \nabla$ and $\sigma \cdot \hat{\mathbf{r}}$, respectively, are the same. In a 3S_1 model the spatial contraction involves $\hat{\mathbf{r}}$ —the unit vector in the relative coordinate of the initial meson’s $q\bar{q}$. In constituent gluon models [17] the spin dependence of the $q\bar{q}$ creation again is via a σ operator, while the spatial contraction depends on the specific model wave functions. In general, for any specific model there will be differing

spatial dependence, but the overall spin coupling coefficients are identical.

Equation (5) expresses full decay amplitudes $a_{j_{12}L}$ as linear combinations of model-dependent spatial amplitudes $A_{l_{12}l_f}$ of the form

$$A_{l_{12}l_f} = \langle ((l_1 \otimes l_2)_{l_{12}} \otimes L)_{l_f} || \nabla || l \rangle. \quad (8)$$

The expansion applies to all partial waves L allowed by the conservation of angular momentum, including those which are parity-forbidden for a given set of spatial quantum numbers. It is the spatial matrix element itself which ensures the conservation of parity; this is verified in the expressions of Ref. [15] where the spatial matrix elements for the production and decay of conventional and hybrid mesons are presented. Thus, for instance, decays of the type ${}^3P_1 \rightarrow {}^1P_1 {}^1S_0$ are allowed in S , P , and D waves, in general; if the initial 3P_1 is a conventional 1^{++} or hybrid 1^{+-} , the S - and D -wave amplitudes vanish, whereas if the initial 3P_1 is a hybrid 1^{-+} the P -wave amplitude vanishes.

The approach taken here, however, is to exploit the relationships between the decay amplitudes $a_{j_{12}L}$, leaving the spatial amplitudes $A_{l_{12}l_f}$ undetermined. These spatial amplitudes depend on the decay momentum and the spatial wave functions; thus, in the limit that the spatial wave functions of the mesons under comparison are the same and the momenta are the same, the expansion of Eq. (5) relates decay amplitudes among families of states sharing the same spatial quantum numbers but having different spin and total angular momentum. If for a given partial wave L there is only one spatial matrix element of the form (8), which we denote A_L , there are direct relations among amplitudes for states with different angular momentum quantum numbers. Three such cases are immediate:

- (1) one of the final states has orbital angular momentum zero ($l_2 = 0$) and the decay is in a relative S -wave ($L = 0$); thus $l_f = l_{12} = l_1$ and the amplitude is expressed in terms of a single matrix element A_S ;
- (2) both final states have orbital angular momentum zero ($l_1 = l_2 = 0$); thus $l_{12} = 0$ and $l_f = L$ and the amplitude in a partial wave L can be expressed in terms of a single matrix element A_L ;
- (3) the initial state and one of the final states have orbital angular momentum zero ($l = l_2 = 0$); thus $l_{12} = l_1$ and $l_f = 1$ and the amplitude in a partial wave L can be expressed in terms of a single matrix element A_L .

We now examine each of these three cases in turn with specific examples. In Sec. II A the S -wave hybrid decays $\pi_1 \rightarrow b_1 \pi$ and $\pi_1 \rightarrow f_1 \pi$ are shown to match results from lattice QCD and thereby to reveal significant information about the underlying dynamics (case 1). In Sec. II B, $a_1 \rightarrow \rho \pi$ and $b_1 \rightarrow \omega \pi$ are examples of case 2; the analysis verifies a conjecture that was made elsewhere [9] and establishes its origin. In Sec. II C case 3 is applied to derive

relations among decays of the type ${}^3S_1 \rightarrow ({}^1P_1; {}^3P_j) + ({}^1S_0; {}^3S_1)$. A new selection rule is derived and the possibility of testing it in the context of e^+e^- annihilation producing flavored and flavorless states is discussed. In Sec. II D we discuss ways of using these results to distinguish hybrid $c\bar{c}$ from 3S_1 or 3D_1 ψ states.

A. S-wave decays of hybrid meson π_1

An immediate example of this factorization is the S -wave decays of the hybrid meson $\pi_1 \rightarrow b_1 \pi$ or $f_1 \pi$. The π_1 has 1^{-+} quantum numbers and $j = s = l = 1$ [5,6]. In flux-tube models and nonrelativistic constituent gluon models [17], the $l = 1$ is explicit; in cavity and bag models it is implicit in the definition of the TE gluon mode which transforms as $\hat{\mathbf{r}} \times \boldsymbol{\epsilon}$ [e.g. see Eq. (2.22) in [18] and applied to hybrid decays in [19]]. The final states have $l_1 = j_1 = 1$ and $s_2 = l_2 = j_2 = 0$, differing in the spin quantum number $s_1 = 0$ (b_1) and $s_1 = 1$ (f_1). For decays in S -wave there is only one matrix element of the form (8), having $l_{12} = l_f = 1$. In the summation over l_{12} and l_f , this constraint is enforced by zeroes in the 9- and 6- j coefficients which reduce to delta functions. This reduces the expansion of Eq. (5) to a simpler form, and the amplitude for the initial state with spin s_1 is given by

$$a_S({}^3P_1 \rightarrow {}^{s_1}P_1 + {}^1S_0) = \frac{3}{\sqrt{2}} \Pi_{s_1} \left\{ \begin{matrix} s_1 & 1 & 1 \\ 1 & 1 & 1 \end{matrix} \right\} \left\{ \begin{matrix} 1/2 & 1/2 & s_1 \\ 1 & 1 & 1/2 \end{matrix} \right\} \times A_S \quad (9)$$

where here A_S is the spatial matrix element. Thus for the 1P_1 and 3P_1 modes

$$a_S({}^3P_1 \rightarrow {}^1P_1 {}^1S_0) = -\frac{A_S}{2\sqrt{3}}, \quad (10)$$

$$a_S({}^3P_1 \rightarrow {}^3P_1 {}^1S_0) = -\frac{A_S}{2\sqrt{6}}. \quad (11)$$

The flavor overlaps for $\pi_1 \rightarrow b_1 \pi$ and $f_1(n\bar{n})\pi$ are $\sqrt{2/3}$ and $\sqrt{1/3}$, so that the ratio of amplitudes is

$$\frac{a_S(\pi_1 \rightarrow b_1 \pi)}{a_S(\pi_1 \rightarrow f_1 \pi)} = 2 \quad (12)$$

which underwrites the result Eq. (1) as found also in lattice QCD. The essential feature here is the factorization of spin and space, and the assumption that the created $q\bar{q}$ are spin triplet. Note that the $q\bar{q}$ creation with quark-spin 1 now appears explicitly in 9- j and 6- j symbols; if the created pair has spin 0 the final 9- j symbol for the πb_1 mode, Eq. (7), has a zero in the bottom left corner, and since

$$\left\{ \begin{matrix} \frac{1}{2} & \frac{1}{2} & 0 \\ \frac{1}{2} & \frac{1}{2} & 0 \\ 0 & 1 & 0 \end{matrix} \right\} = 0 \quad (13)$$

the decay $\pi_1 \rightarrow \pi + b_1(^1P_1)$ would vanish. If spin is conserved, an initial state with $S = 1$ can only decay to a pair of $S = 0$ states if $S = 1$ $q\bar{q}$ is present, hence the need for pair creation to be spin triplet for a nonzero amplitude.

Thus the results of lattice QCD, at least when applied to the decays of a hybrid meson [7], follow if the amplitude factors in space and spin, with the $q\bar{q}$ pair creation being spin triplet and an overall scalar. This does not distinguish 3P_0 from 3S_1 decay models.

B. S- and D-wave decays of axial mesons

Ackleh *et al.* [9] noted that the ratio of the D/S -wave amplitude ratios for $b_1 \rightarrow \omega\pi$ and $a_1 \rightarrow \rho\pi$ can be a sensitive discriminator among models. They found that if the $q\bar{q}$ are created in the 3P_0 configuration, as commonly assumed in flux-tube models, the ratio of D/S ratios is

$$\frac{\frac{a_D}{a_S}(a_1 \rightarrow \rho\pi)}{\frac{a_D}{a_S}(b_1 \rightarrow \omega\pi)} = -\frac{1}{2}. \quad (14)$$

They found the same ratio in the case of $q\bar{q}$ creation by gluon exchange in the static limit (“color coulomb”) but that it departs from $-1/2$ in the case of transverse gluon exchange. It was suggested that this might be useful as a signature of the one-gluon-exchange (OgE) component in the physical decay amplitude, and noted that experimentally the ratio is -0.35 ± 0.09 [9], 2σ away from $-1/2$. Today the ratio

$$\frac{\frac{a_D}{a_S}(a_1 \rightarrow \rho\pi)}{\frac{a_D}{a_S}(b_1 \rightarrow \omega\pi)} = -0.39 \pm 0.06 \quad (15)$$

has a greater precision [20] due to recent experiments [21], though the statistical deviation from $-1/2$ remains similar. Although the authors of Ref. [9] speculated that the common ratio for 3P_0 and coulomb-gluon cases is because of a lack of spin flip, which is violated in the case of transverse gluon exchange and hence the deviation from $-1/2$ in that case, they did not explicitly demonstrate the source.

In the factorization scheme, the amplitude for these decays is proportional to a single matrix element; this is an example of case 2 cited above. Once again, zeroes in the Wigner coefficients reduce the expansion of Eq. (5) to a simpler form and enforce the conservation of angular momentum ($l_{12} = 0$ and $l_f = L$), whereby the amplitude in a partial wave L is proportional to a unique spatial matrix element A_L . The two decay modes of interest differ in the spin quantum number of the initial state, $s = 0$ (b_1) and $s = 1$ (a_1). The amplitudes are given by

$$\begin{aligned} a_L(^sP_1 \rightarrow ^3S_1^1S_0) \\ = \frac{3}{\sqrt{2}}(-)^{L+1}\Pi_s \left\{ \begin{matrix} 1 & s & 1 \\ 1 & L & 1 \end{matrix} \right\} \left\{ \begin{matrix} 1/2 & 1/2 & 1 \\ 1 & s & 1/2 \end{matrix} \right\} \times A_L. \end{aligned} \quad (16)$$

This gives

$$\begin{aligned} a_S(^1P_1 \rightarrow ^3S_1^1S_0) &= -\frac{1}{2\sqrt{3}}A_S, \\ a_D(^1P_1 \rightarrow ^3S_1^1S_0) &= -\frac{1}{2\sqrt{3}}A_D, \end{aligned} \quad (17)$$

$$\begin{aligned} a_S(^3P_1 \rightarrow ^3S_1^1S_0) &= -\frac{1}{\sqrt{6}}A_S, \\ a_D(^3P_1 \rightarrow ^3S_1^1S_0) &= \frac{1}{2\sqrt{6}}A_D. \end{aligned} \quad (18)$$

Thus we have established that the ratio equation (14) is an immediate result of the factorization and $q\bar{q}$ creation with spin 1. A deviation from this ratio is indicative of a breaking of factorization, such as by a transverse gluon which transfers spin and momentum (“spin-orbit coupling”) in general. We shall return to this mechanism for breaking of factorization in Sec. III.

C. S- and D-wave decays of vector mesons

If both of the vector states are 3S_1 , then the decay amplitudes are $V + (0^+, 1^+, 2^+)$, and the amplitudes in S and D waves are each proportional to a unique spatial matrix element A_S, A_D ; this is an example of case 3 discussed earlier. Decays of vector mesons provide a range of tests of factorization and decay dynamics. Decays of the type

$$^3S_1 \rightarrow ^3P_{0,1,2} + ^3S_1, \quad (19)$$

$$^3S_1 \rightarrow ^3P_{1,2} + ^1S_0, \quad (20)$$

$$^3S_1 \rightarrow ^1P_1 + ^3S_1, \quad (21)$$

$$^3S_1 \rightarrow ^1P_1 + ^1S_0 \quad (22)$$

all belong to the special case 3 described earlier; their decay amplitudes in a partial wave L are each proportional to a unique matrix element A_L . Substituting into Eq. (5) $l = 0, s = j = 1$ for the initial state and $l_1 = 1$ and $l_2 = 0$ for the final states gives the amplitude $a_{j_{12}L}$ for the decay in a partial wave L with final states coupled to j_{12} :

$$\begin{aligned} a_{j_{12},L}(^3S_1 \rightarrow ^s_1P_{j_1} + s_2) \\ = \sum_{s_{12}} (-)^{L+j_1+1} \Pi_{1s_1s_2s_{12}s_{12}j_1j_{12}} \left\{ \begin{matrix} s_1 & s_{12} & s_2 \\ j_{12} & j_1 & 1 \end{matrix} \right\} \\ \times \left\{ \begin{matrix} s_{12} & 1 & j_{12} \\ L & 1 & 1 \end{matrix} \right\} \left\{ \begin{matrix} \frac{1}{2} & \frac{1}{2} & s_1 \\ \frac{1}{2} & \frac{1}{2} & s_2 \\ 1 & 1 & s_{12} \end{matrix} \right\} \times A_L. \end{aligned} \quad (23)$$

The results are shown in Table I below. The pattern of amplitudes is realized in specific model calculations that

TABLE I. Decay amplitudes $a_{j_{12}L}$ for the decays (19)–(22).

${}^3S_1 \rightarrow {}^3P_0 {}^3S_1$	$a_{1S} = -A_S/2$ $a_{1D} = 0$
${}^3S_1 \rightarrow {}^3P_1 {}^3S_1$	$a_{1S} = A_S/\sqrt{3}$ $a_{1D} = A_D/4\sqrt{3}$ $a_{2D} = A_D/4$
${}^3S_1 \rightarrow {}^3P_2 {}^3S_1$	$a_{1S} = 0$ $a_{1D} = A_D/4\sqrt{5}$ $a_{2D} = -A_D/4\sqrt{3}$ $a_{3D} = -A_D\sqrt{7/15}$ $a_{3G} = 0$
${}^3S_1 \rightarrow {}^1P_1 {}^3S_1$	$a_{1S} = A_S/\sqrt{6}$ $a_{1D} = -A_D/2\sqrt{6}$ $a_{2D} = -A_D/2\sqrt{2}$
${}^3S_1 \rightarrow {}^1P_1 {}^1S_0$	$a_{1S} = A_S/2\sqrt{3}$ $a_{1D} = A_D/2\sqrt{3}$
${}^3S_1 \rightarrow {}^3P_1 {}^1S_0$	$a_{1S} = A_S/\sqrt{6}$
${}^3S_1 \rightarrow {}^3P_1 {}^1S_0$	$a_{1D} = -A_S/2\sqrt{6}$
${}^3S_1 \rightarrow {}^3P_2 {}^1S_0$	$a_{2D} = A_D/2\sqrt{2}$

have implicitly assumed factorization, e.g. [13], which give explicit expressions for the spatial dependences $A_{S(n)}$ and $A_{D(n)}$ for radial excitations n . The amplitudes in Table I differ from those in Ref. [13] by a phase associated with the ordering of the angular momentum couplings.

1. $\psi(n^3S_1) \rightarrow$ flavored mesons

The results of Table I can be applied immediately to $\psi(n^3S_1) \rightarrow D_{0,2}D^*$ and also to $D_1D^{(*)}$. In the latter case data may be used to determine the mixing angle between 1P_1 and 3P_1 .

The eigenstates for axial flavored mesons are, in general, mixtures of the 3P_1 and 1P_1 states. Reference [22] defines the mixing angles by

$$\begin{aligned} |D_{1L}\rangle &= \cos\phi |{}^1P_1\rangle + \sin\phi |{}^3P_1\rangle, \\ |D_{1H}\rangle &= -\sin\phi |{}^1P_1\rangle + \cos\phi |{}^3P_1\rangle \end{aligned} \quad (24)$$

and discusses ways of determining them experimentally. The amplitudes for axial meson production as a function of mixing angle follow from Table I with careful treatment of phase conventions for the spin-mixed states. Reference [23] adopted the following conventions: for $q\bar{c}$ states (as opposed to $c\bar{q}$ states) and with orbital and spin angular momentum combined in the order $(l \otimes s)_j$, the heavy quark limit gives $\phi = -54.7^\circ$ [23] so that the states are

$$\begin{aligned} |\bar{D}_{1L}\rangle &= \sqrt{\frac{1}{3}} |{}^1P_1\rangle - \sqrt{\frac{2}{3}} |{}^3P_1\rangle, \\ |\bar{D}_{1H}\rangle &= \sqrt{\frac{2}{3}} |{}^1P_1\rangle + \sqrt{\frac{1}{3}} |{}^3P_1\rangle. \end{aligned} \quad (25)$$

The amplitudes of Eq. (5), shown in Table I, are for the topology in which the created q (\bar{q}) ends up in the meson with quantum numbers $s_1 l_1 j_1$ ($s_2 l_2 j_2$). If the axial states are labeled with the quantum numbers $s_1 l_1 j_1$, they are $q\bar{c}$ states in accordance with conventions of Ref. [23]. However, the conventions in the present paper are that amplitudes apply to meson spin coupling in the order $(s \otimes l)_j$, so there is a relative minus sign associated with the 3P_1 part of the amplitude. Thus for the mixed \bar{D}_{1H} , \bar{D}_{1L} states in the heavy quark limit, the amplitudes for ${}^3S_1 \rightarrow \bar{D}_{1L}D$, $\bar{D}_{1H}D$ are

$$\begin{aligned} a_{j_{12}L}({}^3S_1 \rightarrow \bar{D}_{1L}D) &= \sqrt{\frac{1}{3}} a_{j_{12}L}({}^3S_1 \rightarrow {}^1P_1 {}^1S_0) \\ &\quad + \sqrt{\frac{2}{3}} a_{j_{12}L}({}^3S_1 \rightarrow {}^3P_1 {}^1S_0), \end{aligned} \quad (26)$$

$$\begin{aligned} a_{j_{12}L}({}^3S_1 \rightarrow \bar{D}_{1H}D) &= \sqrt{\frac{2}{3}} a_{j_{12}L}({}^3S_1 \rightarrow {}^1P_1 {}^1S_0) \\ &\quad - \sqrt{\frac{1}{3}} a_{j_{12}L}({}^3S_1 \rightarrow {}^3P_1 {}^1S_0), \end{aligned} \quad (27)$$

and likewise for ${}^3S_1 \rightarrow \bar{D}_{1L}D^*$, $\bar{D}_{1H}D^*$. This gives the relative decay widths (up to phase space corrections) shown in Table II below.

Hence in the heavy quark limit

$$\Gamma(\psi(n^3S_1) \rightarrow D^*D_{1L}) = 2\Gamma(\psi(n^3S_1) \rightarrow DD_{1L}), \quad (28)$$

$$\Gamma(\psi(n^3S_1) \rightarrow D^*D_{1H}) = 2\Gamma(\psi(n^3S_1) \rightarrow DD_{1H}), \quad (29)$$

as well as

$$\Gamma(\psi(n^3S_1) \rightarrow D^*D_{1L}) = 2\Gamma(\psi(n^3S_1) \rightarrow D^*D_0), \quad (30)$$

$$\Gamma(\psi(n^3S_1) \rightarrow D^*D_{1H}) = \frac{1}{2}\Gamma(\psi(n^3S_1) \rightarrow D^*D_2), \quad (31)$$

$$\Gamma(\psi(n^3S_1) \rightarrow DD_{1H}) = \Gamma(\psi(n^3S_1) \rightarrow DD_2). \quad (32)$$

In addition there is a selection rule that the D_2 is produced only in helicity 0 or 1; i.e denoting helicity states by 0, (\pm), ($\pm\pm$) then

$$a(\psi(n^3S_1) \rightarrow \bar{D}_2(\pm\pm)D^*(\mp)) = 0. \quad (33)$$

This will be derived in the next section.

TABLE II. Relative widths ${}^3S_1 \rightarrow D^*D_{0,1,2}$ or $DD_{0,1,2}$; the states $D_{1L,H}$ are light and heavy axial mesons in the heavy quark limit.

	S^2	D^2
D_0D^*	1	0
$D_{1L}D^*$	2	0
$D_{1H}D^*$	0	1
D_2D^*	0	2
$D_{1L}D$	1	0
$D_{1H}D$	0	$\frac{1}{2}$
D_2D	0	$\frac{1}{2}$

2. Helicity selection rule

In the factorization scheme, the decay of a transversely polarized ${}^3S_1 \rightarrow {}^3P_2 + {}^3S_1$, with the tensor meson maximally polarized along the decay axis, is predicted to vanish:

$$a({}^3S_1(+)\rightarrow{}^3P_2(++){}^3S_1(-))=0. \quad (34)$$

This selection rule is a test of factorization; a significant nonzero strength for this helicity amplitude in a decay $1^{--} \rightarrow 1^{--}2^{++}$ signals either a breakdown of factorization or the presence of 3D_1 in 1^{--} or of 3F_2 in 2^{++} . The origin of the selection rule is most transparent if we consider the helicity amplitude structure directly. Its generality can then be assessed by transforming to partial wave amplitudes.

First consider the helicity picture. The decay is

$$q_1\bar{q}_4 \rightarrow [q_1\bar{q}_2] + [q_3\bar{q}_4] \quad (35)$$

through the creation of \bar{q}_2q_3 (Fig. 1). Denoting fermions with $S_z = \pm 1/2$ by u, d , respectively, the initial ${}^3S_1(+)$ has its $q\bar{q}$ spins oriented u_1u_4 . The final ${}^3P_2(++){}^3S_1(-)$ then has to be $[u_1\bar{u}_2] + [d_3\bar{d}_4]$ with the $[u_1\bar{u}_2]$ also having $L_z = +1$. For either configuration, spin flip is required for a nonvanishing amplitude.

Spin conservation on spectator lines following the steps above, or the diagrammatic techniques of Ref. [9], enables relations among helicity amplitudes to be calculated in such factorizing models.

In order to expose the more general dynamics underpinning this selection rule, and to exhibit the relations among the various helicity amplitudes, it is useful to transform between helicity and partial wave amplitudes. As before, consider a state with spin j decaying to two particles with spins, respectively, j_1, j_2 . The final state can be characterized by quantum numbers (j_{12}, L) or by helicity quantum numbers (λ_1, λ_2) ; the translation between the two bases, for an initial state with spin projection m along some axis, is given by

$$|jm; \lambda_1, \lambda_2\rangle = \sum_{Lj_{12}} \sqrt{\frac{2L+1}{2j+1}} \langle j_{12}\lambda | j_1\lambda_1; j_2-\lambda_2 \rangle \times \langle j\lambda | j_{12}\lambda; L0 \rangle |jm; j_{12}L\rangle. \quad (36)$$

This enables helicity amplitudes $a_{\lambda_1\lambda_2}$ to be written as

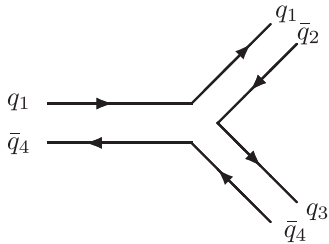


FIG. 1. Strong decay topology.

linear combinations of partial wave amplitudes $a_{j_{12}L}$. We are interested here in decays of the type

$$V(\lambda) \rightarrow \chi_{j_1}(\lambda_1) + V(-\lambda_2) \quad (37)$$

with $\lambda_1 - \lambda_2 = \lambda$; the relation between helicity and partial wave amplitudes follows from (35) above with $j = j_2 = 1$,

$$a_{\lambda_1\lambda_2} = \sqrt{\frac{1}{3}} \langle 1\lambda | j_1\lambda_1; 1-\lambda_2 \rangle a_{1S} + \sqrt{\frac{2}{3}} \sum_{j_{12}} \langle 1\lambda | j_{12}\lambda; 20 \rangle \langle j_{12}\lambda | j_1\lambda_1; 1-\lambda_2 \rangle a_{j_{12}D} + \sqrt{3} \langle 1\lambda | 3\lambda; 40 \rangle \langle 3\lambda | j_1\lambda_1; 1-\lambda_2 \rangle a_{3G}. \quad (38)$$

The resulting relations are shown in the first column of Table III. These relations apply generically to the decay of any vector meson to any scalar, axial, or tensor meson χ_{j_1} . For decays of the type

$${}^3S_1(\lambda) \rightarrow {}^3P_{j_1}(\lambda_1) + {}^3S_1(-\lambda_2), \quad (39)$$

where each of the vectors are explicitly in a 3S_1 state and the χ_{j_1} is a ${}^3P_{j_1}$ state, the amplitude is obtained by substituting for $a_{j_{12}L}({}^3S_1 \rightarrow {}^3P_{j_1} {}^3S_1)$ from Table I; the results are shown in the second column of Table III. The selection rule (33) is explicit in the last line of Table III and follows immediately substituting

$$a_{1S} = a_{3G} = 0; \quad a_{1D} = A_D/4\sqrt{5}; \quad (40) \\ a_{2D} = -A_D/4\sqrt{3}; \quad a_{3D} = -A_D\sqrt{7/15}.$$

The amplitude $a_{3G} \equiv 0$ in 3P_0 or 3S_1 models since $(l_{12} = l_2 = 1) \otimes (L = 3)$ can couple to $(l_f = 2, 3, 4)$, which cannot couple to the $l = 0$ initial state by the vector decay operators ∇ or $\hat{\mathbf{r}}$. The appearance of this zero can be tested by measurement of the various helicity amplitudes which satisfy the linear relation

$$a_{0,0} - 2/\sqrt{3}a_{+,0} + 2/\sqrt{3}a_{+,-} = a_{0,+} + 1/\sqrt{6}a_{+,-}. \quad (41)$$

The selection rule $V(+) \rightarrow T(++)V(-) = 0$ can be violated by failure of factorization, such as when single-gluon exchange produces the \bar{q}_2q_3 and flips spin such as $u_1 \rightarrow d_1$, or if there are 3D_1 admixtures in the wave functions of the produced or initiating vector mesons. The general property that breaks factorization and mixes 3D_1 components in the produced vector meson is essentially the same: in models, the latter is generated by spin-orbit coupling, such as from gluon exchange [24]. To the extent that vector mesons and e^+e^- annihilation are dominated by 3S_1 configurations, and the strong decay amplitude factorizes, the selection rule will apply. For the $\psi(4415)$, which is consistent with being $4{}^3S_1$ [25], the decays $\psi(4415) \rightarrow DD_2$ have been observed by initial state radiation [26]; our selection rule may be testable on the high

TABLE III. Column 1 expresses helicity amplitudes $a_{\lambda_1\lambda_2}$ in terms of partial wave amplitudes $a_{j_{12}L}$ for decays (37) of generic vector states. Column 2 expresses helicity amplitudes in terms of spatial amplitudes A_L for decays (39) with explicit s and l quantum numbers.

	$V(\lambda) \rightarrow \chi_{j_1}(\lambda_1) + V(-\lambda_2)$	${}^3S_1(\lambda) \rightarrow {}^3P_{j_1}(\lambda_1) + {}^3S_1(-\lambda_2)$
$j_1 = 0$	$a_{0,0} = a_{1S}/\sqrt{3} - a_{1D}\sqrt{2/3}$	$= -A_S/2\sqrt{3}$
	$a_{0,+} = a_{1S}/\sqrt{3} + a_{1D}/\sqrt{6}$	$= -A_S/2\sqrt{3}$
$j_1 = 1$	$a_{0,0} = 0$	$= 0$
	$a_{+,0} = a_{1S}/\sqrt{6} + a_{1D}/\sqrt{12} - a_{2D}/2$	$= A_S/3\sqrt{2} - A_D/12$
	$a_{0,+} = -a_{1S}/\sqrt{6} - a_{1D}/\sqrt{12} - a_{2D}/2$	$= -A_S/3\sqrt{2} - A_D/6$
	$a_{+,-} = a_{1S}/\sqrt{6} - a_{1D}/\sqrt{3}$	$= A_S/3\sqrt{2} - A_D/12$
$j_1 = 2$	$a_{0,0} = -a_{1S}\sqrt{2/15} + 2a_{1D}/\sqrt{15} + 3a_{3D}/\sqrt{35} - 2a_{3G}\sqrt{3/35}$	$= -A_D/2\sqrt{3}$
	$a_{+,0} = -a_{1S}/\sqrt{10} - a_{1D}/\sqrt{20} - a_{2D}/\sqrt{12} + 4a_{3D}/\sqrt{105} + 2a_{3G}/\sqrt{35}$	$= -A_D/4$
	$a_{0,+} = a_{1S}/\sqrt{30} + a_{1D}/\sqrt{60} + a_{2D}/2 + 2a_{3D}/\sqrt{35} + a_{3G}\sqrt{3/35}$	$= -A_D/2\sqrt{3}$
	$a_{+,-} = a_{1S}/\sqrt{10} - a_{1D}/\sqrt{5} + a_{3D}\sqrt{3/35} - 2a_{3G}/\sqrt{35}$	$= -A_D/4$
	$a_{+,-} = a_{1S}/\sqrt{5} + a_{1D}/\sqrt{10} - a_{2D}/\sqrt{6} + a_{3D}\sqrt{2/105} + a_{3G}/\sqrt{70}$	$= 0$

mass side of the $\psi(4415)$ in its decays to the low mass tails of $D^*(2010)$ and $D_2(2460)$, respectively. It can also be tested in the e^+e^- continuum immediately around 4.5 GeV, as 3D_1 contamination is expected to be minimal [25].

D. Hybrid and exotic charmonium

While 3S_1 ψ states are expected to dominate the couplings to e^+e^- annihilation, there are local $c\bar{c}$ resonance structures in the 4–5 GeV energy range whose structure is still unestablished [25]. In particular, there are the enigmatic structures $Y(4260)$ and $Y(4325)$ [27]. These have no natural assignment within $c\bar{c}$ spectroscopy, and explanations include hybrid charmonium, or molecules (e.g. by either $cq\bar{c}\bar{q}$ tetraquarks or DD_1 and D^*D_0 attractive forces via π exchange), or even effects associated with S -wave charmed meson thresholds [28].

These states are near the S -wave thresholds for DD_1 , $D^*D_{0,1,2}$. Such decays are an example of case 1 discussed earlier: each S -wave amplitude is proportional to a single spatial matrix element. The coefficient is a function of the spin and orbital angular momenta of the vector initial state, and thus the pattern among decay amplitudes differs for

TABLE IV. Relative S -wave amplitudes for vector charmonia decays with 3S_1 , 3D_1 and ${}^1\Pi_1$ (hybrid) configurations; the states D_{1L} , D_{1H} refer to axial mesons in the heavy quark limit.

	3S_1	3D_1	${}^1\Pi_1$
D_0D^*	$-1/2$	0	$1/3\sqrt{2}$
$D_1({}^1P_1)D^*$	$1/\sqrt{6}$	$-1/2\sqrt{6}$	$1/2\sqrt{3}$
$D_1({}^3P_1)D^*$	$1/\sqrt{3}$	$1/4\sqrt{3}$	$1/2\sqrt{6}$
D_2D^*	0	$1/4\sqrt{5}$	$-\frac{1}{6}\sqrt{\frac{5}{2}}$
$D_1({}^1P_1)D$	$1/2\sqrt{3}$	$1/2\sqrt{3}$	0
$D_1({}^3P_1)D$	$1/\sqrt{6}$	$-1/2\sqrt{6}$	$-1/2\sqrt{3}$
$D_{1L}D$	$1/2$	0	$-1/3\sqrt{2}$
$D_{1H}D$	0	$1/2\sqrt{2}$	$1/6$

3S_1 , 3D_1 and hybrid interpretations, where for the latter the $c\bar{c}$ have $l = 1$ and $s = 0$. Equation (5) gives the coefficient of the spatial matrix element, and the results are shown in Table IV. For axial mesons the amplitudes are shown in both the ${}^1P_1 - {}^3P_1$ basis and in the heavy quark limit, where for the latter the amplitudes are given by Eqs. (26) and (27) and their analogues.

If production of charmed mesons in the decays of 3S_1 $c\bar{c}$ is confirmed to factorize, then using Table IV the relative decay amplitudes to DD_1 , $D^*D_{0,1,2}$ may be used to determine the structure of $c\bar{c}$ states that are near the S -wave thresholds. In particular, this applies to $Y(4260)$ and $Y(4325)$. There are characteristic zeroes that may occur for vector meson decays:

$$\Gamma({}^3S_1 \rightarrow D_{1H}D) = 0, \quad (42)$$

$$\Gamma({}^3D_1 \rightarrow D_{1L}D) = 0, \quad (43)$$

$$\Gamma({}^1\Pi_1(\text{hybrid}) \rightarrow D_1({}^1P_1)D) = 0. \quad (44)$$

The first pair of zeroes arise from the affinity of light and heavy D_{1L} , D_{1H} for S and D couplings, respectively, and the zero (42) was noted by Ref. [25]. For the hybrid decay the result follows from the conclusion of lattice QCD, Sec. II A, that decays are driven by $q\bar{q}$ creation in spin triplet, which implies that a pair of spin singlets (such as D and 1P_1) cannot be produced from a spin singlet, such as a hybrid vector $c\bar{c}$. In practice, these predictions will be affected by mixing, which can be determined from other processes (e.g. see [22]), and by phase space. The relative rates are insensitive to form factor effects at low momenta (see, for example, Refs. [12,13,22]).

III. ELECTRON-POSITRON ANNIHILATION

We consider now the production of meson pairs in e^+e^- annihilation, supposing that such processes proceed

through the strong decay of a virtual quarkonia state $e^+e^- \rightarrow q_1\bar{q}_4 \rightarrow q_1\bar{q}_2 + q_3\bar{q}_4$. An analogous model for ψ decays to light flavor meson pairs was found to be consistent with data assuming the $q_1\bar{q}_4$ state is some radial excitation $n\ ^3S_1$ [29]. If the same applies here, the relative production amplitudes of $^1P_1\ ^1S_0$, $^1P_1\ ^3S_1$, $^3P_j\ ^1S_0$, $^3P_j\ ^3S_1$ will have the pattern of Table I, independently of n . Such relations apply in the limit of equal momentum decays and provided there is not an unfortunate double conspiracy in which both a single n dominates and a node in its amplitude coincides with the kinematic region of interest. This may be checked by varying q^2 to see if the ratios are stable or vary in an oscillatory or nodal manner. The assumption that the pair $q_1\bar{q}_4$ is dominated by a 3S_1 configuration is reasonable above charm threshold where the coupling $e^+e^- \rightarrow ^3D_1(c\bar{c})$ is theoretically and empirically suppressed [20,25]. The results of Table I then apply immediately to $e^+e^- \rightarrow D^*D_{0,2}$ and also to $D^{(*)}D_1$, which in the latter case may be used to determine the mixing angle between 1P_1 and 3P_1 . While this is strictly true on a 3S_1 ψ resonance, it may also be expected to hold through the 4–5 GeV region of interest where 3S_1 is predicted to dominate the e^+e^- cross section.

Application to $e^+e^- \rightarrow \psi + \chi_j$ also follows if this is dominated by strong flux-tube formation and breaking. We shall argue in Sec. IIIB that this is more likely to be dominated by (perturbative) gluon exchange, which breaks factorization and gives a different pattern of amplitudes than strong flux-tube breaking. Our results may be used to test this hypothesis.

In the case of light flavors the neglect of $e^+e^- \rightarrow ^3D_1(q\bar{q})$ is more questionable. The leptonic widths of $^3D_1(q\bar{q})$ are nonetheless expected to be relatively small [30], and empirically the known vector mesons appear to fit well with (radially excited) 3S_1 with some mixing with hybrid vectors without the need for significant 3D_1 [31]. This is clearly an area whose phenomenology merits further clarification. To that end we apply our results with 3S_1 dominance to light flavors in hopes of shedding further light on this sector and isolating 3D_1 states. For ψ decays this simple assumption appears to be consistent with existing data [20,32].

A. $e^+e^- \rightarrow$ flavorless mesons

In the case of $e^+e^- \rightarrow$ neutral states, charge conjugation restricts the production of axial-vector mesons in association with 0^{-+} or 1^{--} to $e^+e^- \rightarrow V + ^3P_1$ or $^1S_0 + ^1P_1$. The amplitudes of Table I apply, and the relative rates then follow by application of Eq. (5):

$$\begin{aligned} & ^3S_1 + ^3P_0 : ^3S_1 + ^3P_1 : ^3S_1 + ^3P_2 : ^1S_0 + ^1P_1 \\ & = 3S^2 : 4S^2 + D^2 : 6D^2 : S^2 + D^2 \end{aligned} \quad (45)$$

and hence

$$\sigma(^3S_1 + ^3P_1) = \frac{4}{3}\sigma(^3S_1 + ^3P_0) + \frac{1}{6}\sigma(^3S_1 + ^3P_2) \quad (46)$$

together with

$$3\sigma(^1S_0 + ^1P_1) = \sigma(^3S_1 + ^3P_0) + \frac{1}{2}\sigma(^3S_1 + ^3P_2) \quad (47)$$

and their corollary

$$\sigma(^1S_0 + ^1P_1) = \frac{1}{8}\sigma(^3S_1 + ^3P_2) + \frac{1}{4}\sigma(^3S_1 + ^3P_1). \quad (48)$$

Note that necessarily

$$\sigma(e^+e^- \rightarrow ^3S_1 + ^3P_1) > \sigma(e^+e^- \rightarrow ^3S_1 + ^3P_0). \quad (49)$$

For flavored states, the two axial mesons are mixtures of 1P_1 and 3P_1 ; whatever the mixing angle may be, the inequality holds true in the sense that the $^3S_1 + ^3P_0$ production rate cannot exceed those of both the axial mesons. In the case of charge conjugation eigenstates we are restricted to applying it to light flavors or to $e^+e^- \rightarrow \psi + \chi_j$. The former case is less well controlled theoretically, due to relativistic effects and potential contamination from 3D_1 background in e^+e^- annihilation, though the above relations appear to be consistent with data and are discussed in Ref. [32]. One of the central applications of the present paper will be to test these predictions against data on $e^+e^- \rightarrow \psi + \chi_j$ where preliminary indications are that the relation Eq. (49) is violated [33]. This is discussed in Sec. IIIB.

The amplitude $V(-)T(++)$, where T denotes a tensor meson, should also be measured for light flavors where VT modes are prominent, especially in ψ decay. Within the factorization hypothesis and 3S_1 dominance, the Vf_2 cannot be produced with f_2 maximally polarized; $a[e^+e^- \rightarrow V(j_z = -1)f_2(j_z = +2)] = 0$. This may be studied in $e^+e^- \rightarrow 5\pi = 2\pi^+2\pi^-\pi^0$ by isolating the channel ωf_2 ; the ω being a narrow state can enable the angular distribution in the decay $f_2 \rightarrow \pi^+\pi^-$ to be measured. The main background here is the potential contamination from e^+e^- annihilation in the 3D_1 state. Although models and data do not suggest this is significant, nonetheless one cannot rule it out. If the amplitude is empirically found to be small, in accord with the selection rule, one could turn this into an advantage and study the amplitude as a function of q^2 and observe if it turns on in the neighborhood of the predicted 3D_1 resonances around 2.2 GeV [30].

B. Factorization breakdown and preformation by OgE

Data on $e^+e^- \rightarrow \psi + X$ at 10.6 GeV c.m. energy show three prominent enhancements X in $e^+e^- \rightarrow \psi + X$ [33], which are consistent with being the η_c , η'_c and χ_0 . The observed pattern of states appears radically different from what is seen for light flavors; for example, the apparent prominence of $e^+e^- \rightarrow \psi + \chi_0$ with only a hint of χ_1 and much suppressed χ_2 contrasts with light flavors where $e^+e^- \rightarrow \omega f_2$ is clearly seen [20]. This suggests that this process for heavy flavors may be controlled by a production mechanism where factorization is broken.

On theoretical grounds one expects that strong factorization may be overwritten here. In e^+e^- annihilation at $E > 6$ GeV, creation of an initial $c\bar{c}$ leaves up to 3 GeV available. As the $c\bar{c}$ separate, forming a strong flux tube up to $O(1$ fm) long, the energy of $O(1$ GeV) enables light-flavored $q\bar{q}$ to form. This is the familiar dynamics that appears to be realized at low energies for light flavors. In the present example, the most probable circumstance is that the excess energy produces multiple $q\bar{q}$, leading to final states $D\bar{D}\pi\pi\cdots$. The experimental selection on final states $\psi X(c\bar{c})$ isolates an unlikely configuration where the 3 GeV has produced a $c\bar{c}$ exclusively. For the flux tube to grow without splitting until it contains 3 GeV of energy would require it to extend to distances exceeding $\Lambda_{\text{QCD}}^{-1}$. This is exponentially unlikely with increasing energy.

Alternatively the energy can be transmitted through a single gluon which converts to $c\bar{c}$. While this is perturbative and expected to be subdominant for processes involving light flavor creation, the question arises at what energy or for what flavors this dominates over flux-tube breaking. The purpose of this section is to propose ways of answering this by experiment. We make specific reference to $e^+e^- \rightarrow (c\bar{c}) + (c\bar{c})$, as there are emerging data in the form of $e^+e^- \rightarrow \psi + X$.

As momentum flows through the gluon, it can transfer spin or angular momentum between the $c\bar{c}$ to which it is coupled. In general, therefore, we anticipate that factorization will break down.

Reference [9] has considered these matrix elements in the explicit nonrelativistic limit (see Appendix B of Ref. [9], especially Eqs. B5–B7). In that limit the gluon-exchange operation transforms as **S.S** and **L.S** but there is no **S.L** operator (where the first operator refers to the transformation property of the gluon emission and the second operator to that of $q\bar{q}$ creation). Thus in the strict nonrelativistic limit of that model, the $V(-)T(++)$ selection rule would appear to survive for the decay of a 3S_1 vector meson. This is no surprise following the discussion after Eq. (34): nonzero amplitude requires spin flip at the emission vertex and orbital flip at the $c\bar{c}$ creation vertex; while the former occurs in the nonrelativistic limit, the latter does not.

However, in e^+e^- annihilation at $q^2 \equiv E_{\text{c.m.}}^2$, the production of a $c\bar{c}$ allows an **S.L** operator at $O(q^2/m_c^2)$. An explicit calculation of the gluon-exchange contributions to $e^+e^- \rightarrow \psi + \chi_j$ has been made in nonrelativistic QCD in Ref. [34], and a nonvanishing amplitude for $V(-)T(++)$ is found even at threshold, in accord with the discussion above. Threshold is when $q^2 = 16m_c^2$; the amplitudes depend upon $r^2 \equiv 16m_c^2/q^2$. At high energies, where $r^2 \rightarrow 0$, the contribution from $e^+e^- \rightarrow {}^3D_1 \rightarrow c\bar{c}$ will become increasingly important, while for the threshold region, $r^2 \rightarrow 1$, the $e^+e^- \rightarrow {}^3S_1 \rightarrow c\bar{c}$ becomes more dominant.

At the 10.6 GeV c.m. energy of the data [33], $r^2 = 0.28$, and Ref. [34] finds for the OgE contribution to the cross

sections $\sigma(\psi\chi_0:\psi\chi_1:\psi\chi_2) \sim 12:2:3$, which contradicts Eq. (49) based upon factorization and assumption of a 3S_1 initial state. In the threshold limit $r^2 \rightarrow 1$ the analysis simplifies and comparison between the predictions of gluon exchange and factorization becomes sharpest. In this limit the VT amplitudes for the transversely polarized initial state of Ref. [34] satisfy

$$\begin{aligned} a[V(-)T(++)]:a[V(0)T(+)]:a[V(+)T(0)] \\ = 1:1/\sqrt{2}:1/\sqrt{6} \end{aligned} \quad (50)$$

in accord with S -wave dominance and the results of Table III. The relative cross sections from the OgE mechanism for $e^+e^- \rightarrow \psi\chi_{0,1,2}$ in the vicinity of threshold $r^2 \rightarrow 1$ in Ref. [34] become

$$\sigma(\psi\chi_0:\psi\chi_1:\psi\chi_2) \sim 24:2:3. \quad (51)$$

Compared to the results at higher energy, $r^2 = 0.28$, the relative sizes of $\psi\chi_1:\psi\chi_2$ have not changed much, but there is a significant relative enhancement of $\sigma(\psi\chi_0)$ near threshold.

This prediction, that the cross section for $\psi\chi_0$ dominates, contrasts with the results of factorization near threshold. For the 3S_1 initial state in the S -wave region near threshold

$$\sigma(\psi\chi_2) \rightarrow 0, \quad \sigma(\psi\chi_0) = \frac{3}{4}\sigma(\psi\chi_1). \quad (52)$$

Analogously, for a 3D_1 initial state

$$\sigma(\psi\chi_0) \rightarrow 0, \quad \sigma(\psi\chi_1) = \frac{5}{3}\sigma(\psi\chi_2), \quad (53)$$

which is also utterly unlike the OgE predictions. Finally one may allow for a coherent mixture of 3S_1 and 3D_1 initial states. Results become model dependent but $\sigma(\psi\chi_0)$ cannot be made larger than both $\sigma(\psi\chi_1)$ and $\sigma(\psi\chi_2)$. Thus in the region of threshold there appear to be marked differences in the expectations of factorization, Eqs. (52) and (53) and OgE Eq. (51).

As one increases energy above threshold, for the 3S_1 initial state, the D -wave decay enables $\sigma(\psi\chi_2)$ to turn on but with the amplitude $a[V(-)T(++)] = 0$ or at least small compared to $a[V(0)T(++)]$ and $a[V(+)T(0)]$. This also contrasts with the predictions from OgE where the $[V(-)T(++)]$ amplitude is the largest for VT production, Eq. (50). A possible contamination comes from $e^+e^- \rightarrow {}^3D_1 \rightarrow c\bar{c}$ contributions which may not be negligible at 6–7 GeV c.m. energies. The S -wave decay amplitudes from initial 3S_1 , 3D_1 and also from hybrid vector mesons are compared in Table IV. Above threshold where D -wave decays are important and ${}^3S_1 - {}^3D_1$ mixing is allowed, results are highly model dependent. While it may be possible to force $\sigma(\psi\chi_0)$ to dominate by a suitable choice of mixing angle, this is not expected to hold true as a function of q^2 .

Thus if dominance of $\psi\chi_0$ is confirmed over a range of q^2 away from threshold, this would support OgE as the

dominant decay mechanism. Conversely, if data near threshold confirm $a[V(-)T(++)] \rightarrow 0$, this would signal factorization being dominant. In any event, we anticipate that the relative populations and helicity structures of $\psi\chi_j$ will vary with q^2 . We recommend that this be investigated in e^+e^- annihilation at super-B factories by means of initial state radiation to access a range of energies. In particular, experiment should attempt to measure the spin dependence of $e^+e^- \rightarrow \psi\chi_2$ as a function of q^2 and compare with the analogous amplitudes in $e^+e^- \rightarrow \omega f_2$.

IV. CONCLUSION

The factorization property of strong decay triggered by $q\bar{q}$ creation in spin triplet, as revealed by lattice QCD, merits further testing. This general feature leads to relations among amplitudes, which can be used as further tests of this dynamics and to determine the nature of participating mesons. Thus we have identified the following tests.

- (1) $\psi(n^3S_1)$ decays or e^+e^- annihilation in the 4–5 GeV energy range will not produce D^*D_2 with the tensor meson in helicity 2. This tests whether the dynamics revealed by lattice QCD for light mesons applies more generally for the strong creation of light flavors.
- (2) If confirmed, then the production $e^+e^- \rightarrow D^{(*)}D_1$ may be used to determine the axial meson mixing angles in the $^3P_1 - ^1P_1$ bases.
- (3) If the mixing angles are known from elsewhere, the pattern of charm pair production can identify the nature of the decaying ψ state. This has an application of immediate relevance in determining the na-

ture of the enigmatic charmoniumlike structures $Y(4260)$ and $Y(4325)$ and also of $\psi(4415)$. Determining whether the $c\bar{c}$ content of these states is $S = 0$ (as for a hybrid) or $S = 1$ then follows from the relative production rates of various combinations of charmed mesons, in particular, of their DD_1 branching ratios.

- (4) The application to light flavors in e^+e^- is less solid, but measurement of the ωf_2 amplitudes as a function of q^2 may isolate 3D_1 resonances in the e^+e^- channel.
- (5) For the creation of heavy flavors, as in $e^+e^- \rightarrow \psi\chi_j$, empirical and theoretical arguments suggest that production is dominated by a single hard gluon rather than the factorization mechanism. The apparent excess of $\psi\chi_0$ and absence of $\psi\chi_2$ needs establishing. We expect that the pattern of χ_j states and their helicity amplitudes will vary significantly with q^2 . We identify the threshold region $e^+e^- \rightarrow \psi\chi_j$ between 6.5 and 7.5 GeV as particularly promising for determining the relative importance of single hard gluon and strong factorization for heavy flavors.

ACKNOWLEDGMENTS

We are grateful to E. Swanson for discussions. This work is supported, in part, by grants from the Science and Technology Facilities Council, the Oxford University Clarendon Fund and the EU-TMR program ‘‘Eurodice,’’ HPRN-CT-2002-00311.

-
- [1] G. S. Bali, K. Schilling, A. Hulsebos, A. C. Irving, C. Michael, and P. W. Stephenson (UKQCD Collaboration), Phys. Lett. B **309**, 378 (1993); C. J. Morningstar and M. J. Peardon, Phys. Rev. D **60**, 034509 (1999).
 - [2] P. Lacock, C. Michael, P. Boyle, and P. Rowland (UKQCD Collaboration), Phys. Lett. B **401**, 308 (1997).
 - [3] N. Isgur and J. E. Paton, Phys. Rev. D **31**, 2910 (1985).
 - [4] T. Barnes, F. E. Close, and E. S. Swanson, Phys. Rev. D **52**, 5242 (1995).
 - [5] N. Isgur, R. Kokoski, and J. E. Paton, Phys. Rev. Lett. **54**, 869 (1985).
 - [6] F. E. Close and P. R. Page, Nucl. Phys. **B443**, 233 (1995).
 - [7] C. McNeile and C. Michael, Phys. Rev. D **73**, 074506 (2006).
 - [8] T. J. Burns and F. E. Close, Phys. Rev. D **74**, 034003 (2006).
 - [9] E. S. Ackleh, T. Barnes, and E. S. Swanson, Phys. Rev. D **54**, 6811 (1996).
 - [10] H. J. Melosh, Phys. Rev. D **9**, 1095 (1974); A. J. G. Hey and J. Weyers, Phys. Lett. **48B**, 69 (1974); F. E. Close and F. J. Gilman, Phys. Lett. **38B**, 541 (1972); F. E. Close, H. Osborn, and A. M. Thomson, Nucl. Phys. **B77**, 281 (1974); F. E. Close, *Introduction to Quarks and Partons* (Academic Press, New York, 1979), Chap. 7.
 - [11] V. Burkert and T. Lee, in *Electromagnetic Interactions and Hadronic Structure*, edited by F. E. Close, A. Donnachie, and G. Shaw (Cambridge University Press, Cambridge, England, 2007), Chap. 3.
 - [12] A. Le Yaouanc, L. Oliver, O. Pene, and J. C. Raynal, Phys. Rev. D **8**, 2223 (1973); G. Busetto and L. Oliver, Z. Phys. C **20**, 247 (1983); R. Kokoski and N. Isgur, Phys. Rev. D **35**, 907 (1987); P. Geiger and E. S. Swanson, Phys. Rev. D **50**, 6855 (1994); H. G. Blundell and S. Godfrey, Phys. Rev. D **53**, 3700 (1996).
 - [13] T. Barnes, F. E. Close, P. R. Page, and E. S. Swanson, Phys. Rev. D **55**, 4157 (1997).
 - [14] P. R. Page, E. S. Swanson, and A. P. Szczepaniak, Phys. Rev. D **59**, 034016 (1999).
 - [15] T. J. Burns, arXiv:hep-ph/0611132.
 - [16] R. Bonnaz and B. Silvestre-Brac, Few-Body Syst. **27**, 163

- (1999).
- [17] A. Le Yaouanc, L. Oliver, O. Pene, J. C. Raynal, and S. Ono, *Z. Phys. C* **28**, 309 (1985); F. Iddir, A. Le Yaouanc, L. Oliver, O. Pene, J. C. Raynal, and S. Ono, *Phys. Lett. B* **205**, 564 (1988); F. Iddir and L. Semmla, arXiv:0710.5352.
- [18] T. Barnes, F. E. Close, and S. Monaghan, *Nucl. Phys. B* **198**, 380 (1982).
- [19] T. Barnes and F. E. Close, *Phys. Lett.* **116B**, 365 (1982); T. Barnes, F. E. Close, F. de Viron, and J. Weyers, *Nucl. Phys.* **B224**, 241 (1983); M. S. Chanowitz and S. R. Sharpe, *Nucl. Phys.* **B222**, 211 (1983); **B228**, 588(E) (1983).
- [20] W. M. Yao *et al.* (Particle Data Group), *J. Phys. G* **33**, 1 (2006).
- [21] M. Nozar *et al.* (E852 Collaboration), *Phys. Lett. B* **541**, 35 (2002); S. U. Chung *et al.*, *Phys. Rev. D* **65**, 072001 (2002).
- [22] F. E. Close and E. S. Swanson, *Phys. Rev. D* **72**, 094004 (2005).
- [23] E. S. Swanson, *Phys. Rep.* **429**, 243 (2006).
- [24] N. Isgur and G. Karl, *Phys. Rev. D* **19**, 2653 (1979); **23**, 817(E) (1981).
- [25] T. Barnes, S. Godfrey, and E. S. Swanson, *Phys. Rev. D* **72**, 054026 (2005); T. Barnes, arXiv:hep-ph/0406327.
- [26] G. Pakhlova *et al.* (Belle Collaboration), arXiv:0708.3313 [*Phys. Rev. D* (to be published)].
- [27] B. Aubert *et al.* (BABAR Collaboration), *Phys. Rev. Lett.* **95**, 142001 (2005); B. Aubert *et al.* (BABAR Collaboration), *Phys. Rev. Lett.* **98**, 212001 (2007).
- [28] F. E. Close, in *Proceedings of the 5th Flavor Physics and CP Violation Conference (FPCP 2007), Bled, Slovenia, 2007*, p. 020.
- [29] T. J. Burns and F. E. Close, arXiv:hep-ph/0711.3755.
- [30] S. Godfrey and N. Isgur, *Phys. Rev. D* **32**, 189 (1985).
- [31] F. E. Close, A. Donnachie, and Y. Kalashnikova, in *Electromagnetic Interactions and Hadronic Structure* (Cambridge University Press, Cambridge, England, 2007), Chap. 4.
- [32] T. Burns and F. E. Close Hadronic Decays of Charmonium (unpublished).
- [33] K. Abe *et al.*, arXiv:hep-ex/0507019. B. Aubert *et al.* (BABAR Collaboration), *Phys. Rev. D* **72**, 031101 (2005).
- [34] E. Braaten and J. Lee, *Phys. Rev. D* **67**, 054007 (2003); **72**, 099901(E) (2005).